JB
Journals.ASM.org

Conserved Terminal Organelle Morphology and Function in *Mycoplasma penetrans* and *Mycoplasma iowae*

Dominika A. Jurkovic, Jaime T. Newman, and Mitchell F. Balish

Department of Microbiology, Miami University, Oxford, Ohio, USA

Within the genus *Mycoplasma* are species whose cells have terminal organelles, polarized structures associated with cytadherence and gliding motility. *Mycoplasma penetrans*, found mostly in HIV-infected patients, and *Mycoplasma iowae*, an economically significant poultry pathogen, are members of the *Mycoplasma muris* phylogenetic cluster. Both species have terminal organelles that interact with host cells, yet the structures in these species, or any in the *M. muris* cluster, remain uncharacterized. Time-lapse microcinematography of two strains of *M. penetrans*, GTU-54-6A1 and HF-2, and two serovars of *M. iowae*, K and N, show that the terminal organelles of both species play a role in gliding motility, with differences in speed within and between the two species. The strains and serovars also differed in their hemadsorption abilities that positively correlated with differences in motility speeds. No morphological differences were observed between *M. penetrans* and *M. iowae* by scanning electron microscopy (SEM). SEM and light microscopy of *M. penetrans* and *M. iowae* showed the presence of membranous filaments connecting pairs of dividing cells. Breaking of this filament during cell division was observed for *M. penetrans* by microcinematography, and this suggests a role for motility during division. The Triton X-100-insoluble fractions of *M. penetrans* and *M. iowae* consisted of similar structures that were unique compared to those identified in other mycoplasma species. Like other polarized mycoplasmas, *M. penetrans* and *M. iowae* have terminal organelles with cytadherence and gliding functions. The difference in function and morphology of the terminal organelles suggests that mycoplasmas have evolved terminal organelles independently of one another.

Reductive evolution of the bacterial genus *Mycoplasma* from Gram-positive bacteria has resulted in cell wall-less organisms with both reduced genome size and reduced biosynthetic ability. This genus includes both commensals and pathogens and is associated with vertebrate hosts, including humans. For many pathogenic mycoplasmas, a first step in causing disease is adherence to host cells, often by adhesins associated with a polarized organelle (1). The interactions of mycoplasmas with host cells are diverse and complex. *Mycoplasma pneumoniae*, a human pathogen, requires a polar terminal organelle for cytadherence and gliding motility (1), which may be required for colonization of host tissue (13). *Mycoplasma mobile*, a fish pathogen, also has a terminal organelle but with morphology distinct from that of *M. pneumoniae* (1). Although both species have terminal organelles, the proteins involved in biogenesis and function of these polar structures are completely different. For example, *M. pneumoniae* adhesins P1 and P30 are located at the tips and/or sides of the terminal organelle (29), whereas the *M. mobile* adhesin Gli349 is found at the base, or neck, of its terminal organelle (33). The two species also have very different gliding characteristics (11, 25) and distinct internal organizations of their respective polar organelles (3, 23).

Mycoplasma penetrans and *Mycoplasma iowae* are both found in the *Mycoplasma muris* cluster within the pneumoniae group. *M. penetrans* is found commonly in the urogenital tract of HIV-positive individuals (19, 34) but has also been isolated from the blood of a non-HIV-infected individual with antiphospholipid syndrome (35). Previous research has focused on the role of *M. penetrans* in AIDS. Its lipoproteins are mitogenic (5) and stimulate transcription of the HIV genome in HIV-infected cells *in vitro* via Toll-like receptors (30), suggesting that *M. penetrans* may play a role in expediting the progression of AIDS. *M. iowae* is a poultry pathogen isolated from the respiratory tract of turkeys and chickens (36) and the gastrointestinal tract of turkeys (21). In experimental infections, *M. iowae* causes embryo death in turkey (36) and chicken eggs (4). *M. iowae* commercial infections have been identified in turkey poults, resulting in a variety of leg abnormalities (16, 31), which can have a negative impact upon meat production.

Both *M. penetrans* and *M. iowae* exhibit polarity, with a terminal polar organelle mediating adherence to human epithelial cells (19) and colonization of intestinal mucosa in turkeys (21), respectively. The proteins involved in the organization and function of the polar organelle remain unknown in both *M. penetrans* and *M. iowae*; the *M. penetrans* genome lacks homologs of genes involved in terminal organelle structure in *M. pneumoniae* and *M. mobile* (10, 12, 28). Electron microscopy reveals that both species have two distinct cytoplasmic components. The polar organelles of *M. penetrans* and *M. iowae* are densely packed with material of a fine granular structure, compared with the cell body, whose appearance is more typical of bacterial cytoplasm (19, 21). Although it is likely that these organisms utilize a polar organelle to mediate attachment and invade their respective hosts (6), it is unknown whether features typically associated with this structure in other polarized mycoplasmas, including gliding motility and an internal cytoskeleton, are present. Improved understanding of the mechanisms that *M. penetrans* and *M. iowae* use to interact with host cells is hampered by the lack of a genetic manipulation system for use in *M. penetrans* and the lack of a completed genome sequence for *M. iowae*. Despite the availability of a genome

Received 13 January 2012 **Accepted** 18 March 2012
Published ahead of print 23 March 2012
Address correspondence to Mitchell F. Balish, BalishMF@MUOhio.edu.

doi:10.1128/JB.00060-12

TABLE 1 Gliding motility parameters and Triton X-100-insoluble structure dimensions of *M. penetrans* and *M. iowae*

Organism	Speed (range [nm/s])[a]	Cells moving per frame (%)	Length of insoluble structure (nm)[a]	Greatest width of insoluble structure (nm)[a]	Width of insoluble structure across narrow portion (nm)[a]
M. penetrans strain GTU-54-A1	548 ± 217 (151–1,284)	23	449 ± 79	187 ± 60	127 ± 25
M. penetrans strain HF-2	54 ± 18 (25–111)	30	ND	ND	ND
M. iowae serovar N	797 ± 427 (200–2,150)	13	442 ± 54	237 ± 71	109 ± 18
M. iowae serovar K	270 ± 125 (95–621)	8	ND	ND	ND

[a] Values are means ± standard deviations. ND, not determined.

sequence for *M. penetrans*, it is unclear which proteins are associated with its terminal organelle.

Reasoning that, as in other mycoplasmas, polarity in *M. penetrans* and *M. iowae* might be associated with gliding motility and a cytoskeletal structure and that the elements responsible for these properties are likely to be novel, we investigated strains of *M. penetrans* and *M. iowae* by detergent treatment, microscopy, and microcinematography. Both *M. penetrans* and *M. iowae* were found to be motile but with properties that distinguish both organisms from other mycoplasmas. In addition, they share novel, detergent-insoluble structures consistent with a terminal organelle-associated cytoskeletal element. This study expands the known diversity of mycoplasma cell structure and provides insight into interactions between these two species and their respective host cells.

MATERIALS AND METHODS

Bacterial culture conditions. *Mycoplasma penetrans* strains GTU-54-6A1 (18) and HF-2 (35) and *Mycoplasma iowae* serovars N and K (2) were cultured at 37°C in SP-4 broth (32) or on SP-4 agar plates.

Hemadsorption (HA). Plates containing mycoplasma colonies were incubated with sheep red blood cells (SRBC) in Alsever's solution (Cleveland Scientific) and washed with phosphate-buffered saline as previously described (8). Colonies were observed and photographed at a ×400 magnification on a Leica DM IRB inverted phase-contrast/epifluorescence microscope.

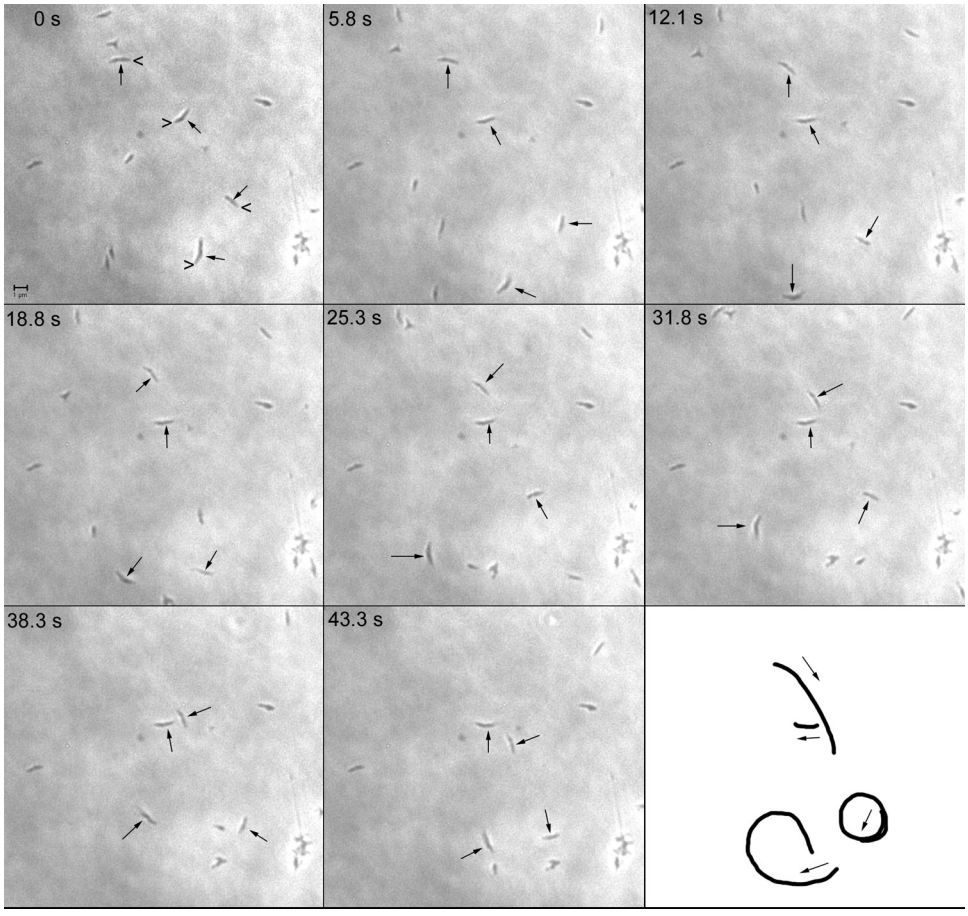

FIG 1 Consecutive phase-contrast images of *M. penetrans* in a chamber slide at intervals of 5 to 6 s at 37°C. Four representative cells are indicated by arrows. In the first frame (0 s), the carets point to the leading ends of gliding cells. In the last frame, the paths of the gliding cells are represented, with arrows indicating the direction of gliding during the observation period. Scale bar, 1 μm.

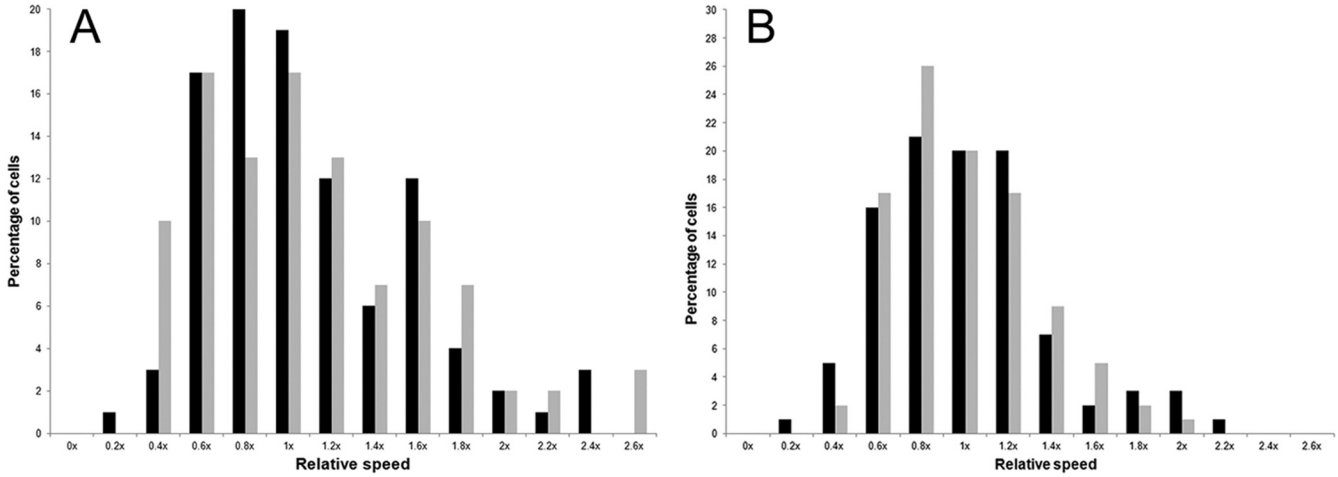

FIG 2 Distribution of mycoplasma gliding velocities about the mean. Gliding speeds of the individual motile cells for each strain or serovar were grouped into bins of 0.2× the mean, designated *x*, for each species. The percentage of cells with speeds in a given range out of the total population of motile cells was plotted against the speed as a fraction of the mean speed for each isolate. (A) Black bars, *M. iowae* serovar K; gray bars, *M. iowae* serovar N. (B) *M. penetrans*. Black bars, strain GTU-54-6A1; gray bars, strain HF-2.

Time-lapse microcinematography. *M. penetrans* and *M. iowae* cells from frozen, mid-log-phase stocks were filtered through a 0.45-μm-pore-size filter and incubated 3 h at 37°C in glass chamber slides (Nunc) in SP-4 broth supplemented with 3% gelatin. In each analysis, 27 images were captured at a ×1,000 magnification on a Leica DM IRB inverted phase-contrast/epifluorescence microscope at intervals ranging from 0.5 to 1 s. Images were merged and analyzed as previously described (8). Gliding speeds of individual cells were calculated by dividing the distance traveled by the number of frames between which cells moved. For each strain, at least 100 motile cells were analyzed.

SEM. Cells were prepared for scanning electron microscopy (SEM) as previously described (8). Briefly, they were grown for 6 h to 1 day in SP-4 broth supplemented with 3% gelatin at 37°C. To analyze Triton X-100-insoluble structures, Triton X-100 in 20 mM Tris-HCl (pH 7.5)–150 mM NaCl was added to whole cells to a final concentration of 1%, and the coverslips were incubated for 30 min at 37°C. Coverslips were fixed for 30 min in 1.5% glutaraldehyde, 1% paraformaldehyde, and 0.1 M sodium cacodylate, pH 7.2, rinsed with buffer, and dehydrated through a series of ethanol washes from 25% to 100%. Following dehydration, the coverslips were critical-point dried and then viewed on a Zeiss Supra 35 FEG-VP scanning electron microscope.

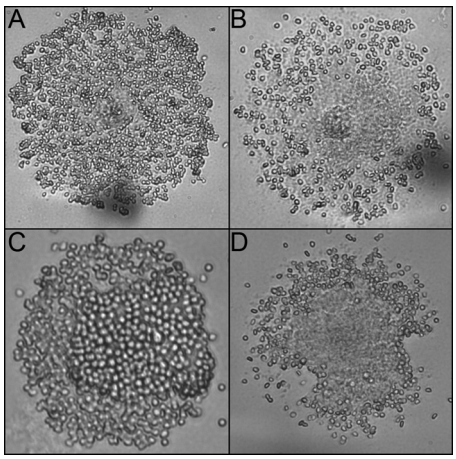

FIG 3 Colony HA of *M. penetrans* and *M. iowae*. (A) *M. penetrans* strain GTU-54-6A1. (B) *M. penetrans* strain HF-2. (C) *M. iowae* serovar K. (D) *M. iowae* serovar N.

Membrane and DNA staining. To visualize cell membranes, cells were grown overnight in 24-well plates on glass coverslips in SP-4 broth supplemented with 3% gelatin at 37°C. Cells were stained with 3,3′-dihexyloxacarbocyanine iodide ($DiOC_6$; Sigma-Aldrich) for 10 min at a final concentration of 5 μg/ml and then fixed directly in the medium using the same fixative as for SEM. To visualize the nucleoid, cells were grown overnight. The medium and fixative were removed, and 4′,6-diamidino-2-phenylindole (DAPI; Sigma-Aldrich) solution was added to the coverslips for 30 min in the dark at a final concentration of 1 μg/ml. Cells were visualized using phase-contrast microscopy. $DiOC_6$ and DAPI were visualized by epifluorescence microscopy using rhodamine and DAPI filter sets, respectively.

RESULTS

Gliding speed and HA. Because *M. penetrans* and *M. iowae* attach via a polar structure (19, 21), we tested whether these organisms exhibited gliding motility, which is characteristic of other mycoplasma species bearing similar structures (1). *M. penetrans* strains GTU-54-6A1 and HF-2 and *M. iowae* serovars N and K were all found to be motile, albeit at distinctly different speeds (Table 1). Consecutive phase-contrast images of *M. penetrans* gliding showed that cells moved in a unidirectional manner, led by one end of the cell (Fig. 1). Cells moved in both straight and curved paths but never reversed direction.

In both species, average gliding speeds were within the range of extremes previously observed for mycoplasma motility, that is, <30 nm/s for *Mycoplasma pirum* and *Mycoplasma insons* and >2,500 nm/s for *Mycoplasma testudinis* and *Mycoplasma mobile* (9, 14, 26). On average, *M. penetrans* strain GTU-54-6A1 glided 10 times faster than strain HF-2, and *M. iowae* serovar N glided 3 times faster than *M. iowae* serovar K. Unlike other motile species in the pneumoniae group, both *M. penetrans* and *M. iowae* exhibited a large range in their average gliding speeds (Table 1; Fig. 2); however, as with *M. insons*, gliding frequency was low. Motility of *M. pneumoniae* ceases around the time of cytokinesis (7), raising the possibility that the low percentages of moving *M. penetrans* and *M. iowae* cells might be attributable to engagement in the cell

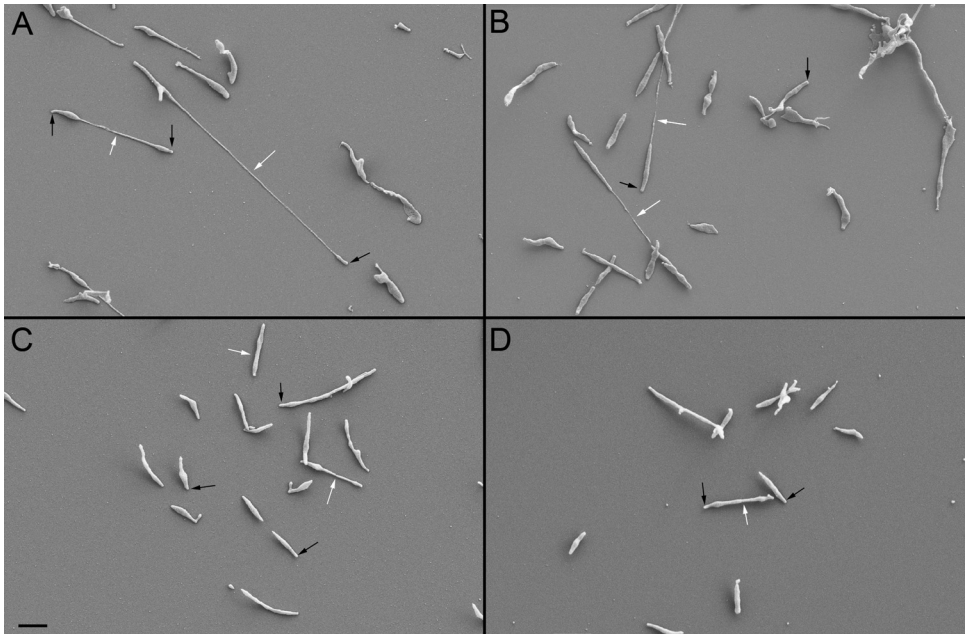

FIG 4 SEM of *M. penetrans* and *M. iowae* cells attached to glass. (A) *M. penetrans* strain GTU-54-6A1. (B) *M. penetrans* strain HF-2. (C) *M. iowae* serovar K. (D) *M. iowae* serovar N. White arrows, filamentous structures connecting individual cell bodies; black arrows, attachment organelles. Scale bar, 1 μm.

division process. Indeed, paired cells were frequently observed (see Fig. 4); individual stationary cells might also have been near cytokinesis. Cells that were clearly dividing (see below) and aggregates or microcolonies of cells were neither analyzed for speed nor enumerated among the total number of cells analyzed.

To test whether isolates differed in cytadherence, we performed HA assays on both *M. penetrans* strains and both *M. iowae* serovars. Both *M. penetrans* strains were HA positive, as previously described for strain GTU-54-6A1 (18), but there was a consistent difference in the coverage of colonies by SRBC. GTU-54-6A1 colonies were completely covered by SRBC (Fig. 3A), but HF-2 colonies were more sparsely covered, with most SRBC binding the colony periphery (Fig. 3B). *M. iowae* serovars N and K were also both HA positive, as previously described (19), and also exhibited differences in SRBC coverage. *M. iowae* serovar N colonies (Fig. 3C) were completely covered with SRBC, whereas *M. iowae* serovar K colonies were covered with SRBC only at the colony peripheries (Fig. 3D). Interestingly, for both species it was the faster-gliding variety that exhibited greater coverage by SRBC, but all isolates were nonetheless HA positive.

Morphology and internal organization of *Mycoplasma penetrans* and *Mycoplasma iowae*. The cell morphologies of glass-attached *M. penetrans* and *M. iowae* cells were observed by SEM. *M. penetrans* (Fig. 4A and B) and *M. iowae* cells (Fig. 4C and D) had similar appearances. Though pleomorphic, cells consisted of an attachment organelle and a cell body. In both species, paired cells were frequently connected by a filament that was continuous with the cell membrane (data not shown) which varied considerably in length. Unfiltered cells had a propensity to form microcolonies, consistent with the aggregates observed during time-lapse microcinematography.

To test whether the filaments connecting cell bodies represented a cytokinesis intermediate, we observed the division of paired *M. penetrans* strain GTU-54-6A1 cells under the same conditions used for analyzing gliding motility (Fig. 5). The filament routinely increased in length and became thinner as the two cells moved away from each other. Eventually the filament snapped, irrespective of either the passage of a constant amount of time or achievement of a particular length. After division, only one cell glided immediately, whereas the second cell remained stationary for a period of time, as was previously observed for *M. pneumoniae* (7). Staining of cells with DAPI revealed that the nucleoid was present in the cell body but absent from the terminal organelle and from the filaments con-

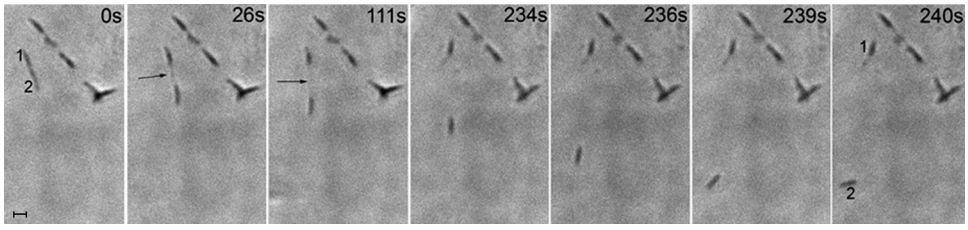

FIG 5 Time-lapse images of dividing *M. penetrans* strain GTU-54-6A1 cells. Times in the panels after the leftmost panel indicate elapsed time from that starting point. Individual members of each dividing pair are numbered in the first and last panels. Arrows, filamentous structures prior to division. Scale bar, 1 μm.

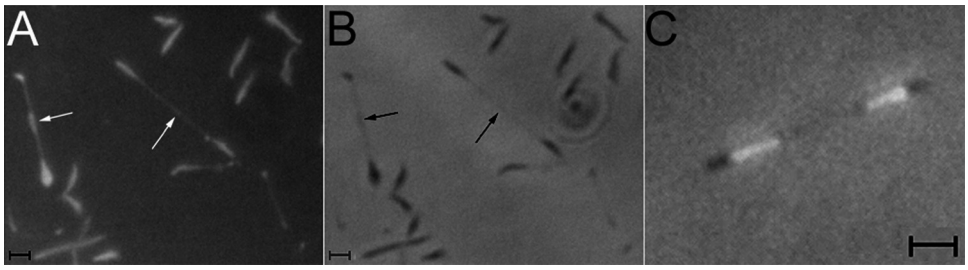

FIG 6 Membrane and nucleoid staining in *M. penetrans* strain GTU-54-6A1. $DiOC_6$ fluorescence (A) and a corresponding phase-contrast image (B) are shown. Arrows, filamentous structures connecting individual cell bodies. (C) White DAPI fluorescence is overlaid onto a phase-contrast image of a pair of dividing cells. Arrowheads, attachment organelles lacking DNA. Scale bar, 1 μm.

necting paired cells (Fig. 6). The edge of the nucleoid adjacent to the terminal organelle was very flat, suggesting the presence of a physical boundary. The average length of the nucleoid-free space in the region of the terminal organelle was 470 ± 60 nm, and the average width adjacent to the nucleoid was 310 ± 80 nm ($n = 32$).

Triton X-100-insoluble structures of *M. penetrans* and *M. iowae*. Since *M. penetrans* and *M. iowae* are both motile and share similar cell morphologies, we treated cells with Triton X-100 to test for the presence of a cytoskeletal structure such as the structures found in the terminal organelles of *M. pneumoniae* (20) and *M. mobile* (23). Treatment of both *M. penetrans* (Fig. 7A) and *M. iowae* (Fig. 7B) with 1% Triton X-100 revealed that both species harbored cylindrical or pear-shaped objects, studded by projections, which dominated the images. These structures were indistinguishable between strains within species, although somewhat distinctive between the two species. There was no significant difference in the lengths of the most consistent structures between the two species at 440 to 450 nm (Table 1), corresponding to the length of the nucleoid-free space in the terminal organelle (see above). Because of the shape of the insoluble structures, width measurements were taken at both the widest point and the point at which the structure begins to narrow. For both width measurements, there was a statistically significant difference (one-way analysis of variance [ANOVA], $P < 0.05$; $n = 25$) between the two species, with *M. iowae* exhibiting greater extremes (Table 1). In addition to these predominant structures, both species also contained Triton X-100-insoluble structures that were distinctly shorter or longer, which might represent intermediates in their assembly.

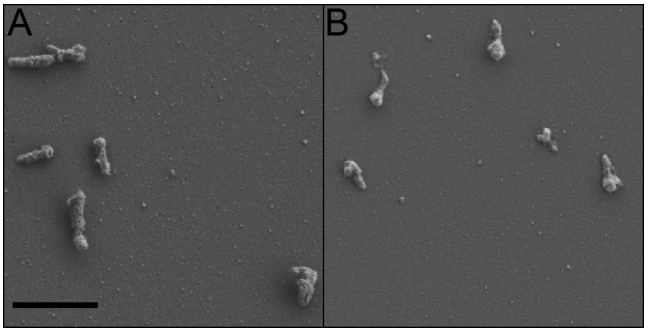

FIG 7 SEM of *M. penetrans* and *M. iowae* cells attached to glass, treated with Triton X-100 detergent. (A) *M. penetrans* strain GTU-54-6A1. (B) *M. iowae* serovar N. Scale bar, 1 μm.

DISCUSSION

Ultrastructure. The role of terminal organelles in mediating both cytadherence and gliding motility has been characterized in several members of the *Mycoplasma* genus (9, 22). *M. penetrans* and *M. iowae* are the first motile species identified in the *M. muris* cluster and increase the number of described motile mycoplasma species to 12, 11 of which have terminal organelles. Despite the close relationship between the *M. muris* and *M. pneumoniae* clusters, the overall ultrastructures of the *M. iowae* and *M. penetrans* terminal organelles differ substantially from the ultrastructure of *M. pneumoniae*. The novel Triton X-100-insoluble structures of *M. penetrans* and *M. iowae* represent a third type of cytoskeletal organization associated with mycoplasma terminal organelles, with *M. pneumoniae* and *M. mobile* representing the first two types. The length of the Triton X-100-insoluble structure of *M. penetrans* is consistent with that of the nucleoid-free space of the terminal organelle, consistent with a model in which it fills that space. The width of the structure, on the other hand, is less than that of the nucleoid-free space, suggesting either that this structure is at the core of a larger structure whose exterior is solubilized during extraction or that dehydration introduces artifacts that reduce the width. It is likely that the densely packed material within the *M. penetrans* polar organelle observed in thin sections (19, 24) is actually this Triton X-100-insoluble structure. Similar material is observed in electron micrographs of *M. iowae* polar organelles (21). The uniform appearance of the densely packed material in these images argues against a second type of structure that was not recovered in our experiments. Further studies are necessary to identify the proteins that comprise both structures as well as their development and function.

Gliding motility. The gliding characteristics of *M. penetrans* and *M. iowae* are distinct from those of other mycoplasma species in particular ways. One is the discontinuity of their movement compared with that of *M. mobile* cells, which rarely rest during motility (27), and with movement of species of the *M. pneumoniae* phylogenetic cluster, which rest more frequently than *M. mobile* (25), but not to the degree observed in *M. penetrans* and *M. iowae*. As a measure of this phenomenon, on average, individual *M. penetrans* strain GTU-54-6A1 cells moved for ~70% of the observation period (data not shown), whereas *Mycoplasma genitalium* strain G37 cells moved for ~90% of the period (J. M. Hatchel and M. F. Balish, unpublished data); in both cases cells that appeared to be impeded were discounted. A second distinctive characteristic is the existence of substantial gliding speed differences among isolates

of *M. penetrans* and *M. iowae* not observed in other species (data not shown). It is unclear whether the differences observed in gliding speed and coverage of colonies by SRBC in the HA assay have any relationship to the sites from which the organisms were isolated. *M. penetrans* strain GTU-54-6A1, isolated from the urogenital tract of HIV-infected individuals (19, 34), glides faster than strain HF-2, which was isolated from the respiratory tract of an HIV-negative person with primary antiphospholipid syndrome (35). Additionally, *M. iowae* serovar N, isolated from the air sac of turkeys (2), glides faster than *M. iowae* serovar K, isolated from the oviduct of chickens. Further comparison of both strains and serovars among *M. penetrans* and *M. iowae* may be helpful in identifying the molecular components associated with adherence and motility in these two species.

Cell division. In *M. penetrans*, we observed a clear relationship between motility and cell division. Dividing cells were connected by cell membrane filaments, which increased in length as the distance between both daughter cells increased over time. The straightness of filaments connecting the cell pairs suggests that the filaments experience tension, most likely the result of the gliding-associated forces generated by the terminal organelles of one or both cells of the pair. The lack of DAPI fluorescence in the filaments of paired cells suggests that the filaments are free of DNA and are formed after nucleoid segregation, in agreement with images in which nonfilamentous individual cells appear to have two distinct nucleoids (data not shown). We observed breakage of filaments at the culmination of cell division, with one cell remaining stationary and the other gliding away. This observation is identical to observations of dividing *M. pneumoniae* cells (7). Like other mycoplasmas, *M. penetrans* may rely at least in part on the force generated by gliding motility for cell division (17).

Independent evolution of mycoplasma terminal organelles. Although terminal organelles in *M. mobile*, the *M. pneumoniae* cluster, and the *M. muris* cluster facilitate the same sets of functions, there are significant disparities in overall terminal organelle organization and protein composition in each of these groups. We believe that these data are irreconcilable with a model in which these structures spring from a common evolutionary origin. The observations here regarding *M. penetrans* and *M. iowae* not only demonstrate the distinct characteristics of members of the *M. muris* cluster but also indicate that comparing more *Mycoplasma* species is critical for gaining a more complete understanding of both the unifying and diverse elements of terminal organelle function and its role in disease caused by any single species.

ACKNOWLEDGMENTS

This work was supported by the National Institutes of Health (Public Health Service grant R15 A1073994) and by the Miami University Doctoral-Undergraduate Opportunities in Scholarship program.

We gratefully acknowledge the following for providing mycoplasma strains: Z. Raviv (The Ohio State University) for *M. iowae* serovars N and K, M. Davidson (Mollicutes Culture Collection, Purdue University) for *M. penetrans* strain GTU-54-6A1, and L. Duffy (University of Alabama-Birmingham) for *M. penetrans* strain HF-2. We thank C. M. Fullem for early work on DAPI staining of *M. penetrans*. We are also grateful to D. Krause (University of Georgia) for reading the manuscript.

REFERENCES

1. **Balish MF.** 2006. Subcellular structures of mycoplasmas. Front. Biosci. **11**:2017–2027.
2. **Barber TL, Fabricant J.** 1971. A suggested reclassification of avian *Mycoplasma* serotypes. Avian Dis. **15**:125–138.
3. **Biberfeld G, Biberfeld P.** 1970. Ultrastructural features of *Mycoplasma pneumoniae*. J. Bacteriol. **102**:855–861.
4. **Bradbury JM, McCarthy JD.** 1983. Pathogenicity of *Mycoplasma iowae* for chick embryos. Avian Pathol. **12**:483–496.
5. **Feng SH, Lo SC.** 1994. Induced mouse spleen B-cell proliferation and secretion of immunoglobulin by lipid-associated membrane proteins of *Mycoplasma fermentans* incognitus and *Mycoplasma penetrans*. Infect. Immun. **62**:3916–3921.
6. **Giron JA, Lange M, Baseman JB.** 1996. Adherence, fibronectin binding and induction of cytoskeleton reorganization in cultured human cells by *Mycoplasma penetrans*. Infect. Immun. **64**:197–208.
7. **Hasselbring BM, Jordan JL, Krause RW, Krause DC.** 2006. Terminal organelle development in the cell wall-less bacterium *Mycoplasma pneumoniae*. Proc. Natl. Acad. Sci. U. S. A. **103**:16478–16483.
8. **Hatchel JM, Balish RS, Duley ML, Balish MF.** 2006. Ultrastructure and gliding motility of *Mycoplasma amphoriforme*, a possible human respiratory pathogen. Microbiology **152**:2181–2189.
9. **Hatchel JM, Balish MF.** 2008. Attachment organelle ultrastructure correlates with phylogeny, not gliding motility properties, in *Mycoplasma pneumoniae* relatives. Microbiology **154**:286–295.
10. **Himmelreich R, et al.** 1996. Complete sequence analysis of the genome of the bacterium *Mycoplasma pneumoniae*. Nucleic Acids Res. **22**:4420–4449.
11. **Jaffe JD, Miyata M, Berg HC.** 2004. Energetics of gliding motility in *Mycoplasma mobile*. J. Bacteriol. **186**:4254–4261.
12. **Jaffe JD, et al.** 2004. The complete genome and proteome of *Mycoplasma mobile*. Genome Res. **8**:1447–1461.
13. **Jordan JL, et al.** 2007. Protein P200 is dispensable for *Mycoplasma pneumoniae* hemadsorption but not gliding motility or colonization of differentiated bronchial epithelium. Infect. Immun. **75**:518–522.
14. **Kirchhoff H, Rosengarten R.** 1984. Isolation of motility mycoplasma from fish. J. Gen. Microbiol. **130**:2439–2445.
15. Reference deleted.
16. **Ley DH, Marusak RA, Vivas EJ, Barnes HJ, Fletcher OJ.** 2010. *Mycoplasma iowae* associated with chondrodystrophy in commercial turkeys. Avian Pathol. **39**:87–93.
17. **Lluch-Senar M, Querol E, Piñol J.** 2010. Cell division in a minimal bacterium in the absence of *ftsZ*. Mol. Microbiol. **78**:278–289.
18. **Lo SC, et al.** 1992. *Mycoplasma penetrans* sp. nov., from the urogenital tract of patients with AIDS. Int. J. Syst. Bacteriol. **42**:357–364.
19. **Lo SC, et al.** 1991. Newly discovered mycoplasma isolated from patients infected with HIV. Lancet **338**:1415–1418.
20. **Meng KE, Pfister RM.** 1980. Intracellular structures of *Mycoplasma pneumoniae* revealed after membrane removal. J. Bacteriol. **144**:390–399.
21. **Mirsalimi SM, Rosendal S, Julian RJ.** 1989. Colonization of the intestine of turkey embryos exposed to *Mycoplasma iowae*. Avian Dis. **33**:310–315.
22. **Miyata M, Uenoyama A.** 2002. Movement on the cell surface of the gliding bacterium, Mycoplasma mobile, is limited to its head-like structure. FEMS Microbiol. Lett. **215**:285–289.
23. **Nakane D, Miyata M.** 2007. Cytoskeletal "jellyfish" structure of *Mycoplasma mobile*. Proc. Natl. Acad. Sci. U. S. A. **104**:19518–19523.
24. **Neyrolles O, et al.** 1998. Identification of two glycosylated components of *Mycoplasma penetrans*: a surface-exposed capsular polysaccharide and a glycolipid fraction. Microbiology **144**:1247–1255.
25. **Radestock U, Bredt W.** 1977. Motility of *Mycoplasma pneumoniae*. J. Bacteriol. **129**:1495–1501.
26. **Relich RF, Friedberg AJ, Balish MF.** 2009. Novel cellular organization in a gliding mycoplasma, *Mycoplasma insons*. J. Bacteriol. **191**:5312–5314.
27. **Rosengarten R, Kirchhoff H.** 1987. Gliding motility of *Mycoplasma* sp. nov. strain 163K. J. Bacteriol. **169**:1891–1898.
28. **Sasaki Y, et al.** 2002. The complete genomic sequence of *Mycoplasma penetrans*, an intracellular bacterial pathogen in humans. Nucleic Acids Res. **30**:5293–5300.
29. **Seto S, Miyata M.** 2003. Attachment organelle formation represented by localization of cytadherence proteins and formation of the electron-dense core in wild-type and mutant strains of *Mycoplasma pneumoniae*. J. Bacteriol. **185**:1082–1091.
30. **Shimizu T, Kida Y, Kuwano K.** 2004. Lipid-associated membrane proteins of *Mycoplasma fermentans* and *M. penetrans* activate human immu-

nodeficiency virus long-terminal repeats through Toll-like receptors. Immunology **113**:121–129.
31. **Trampel DW, Frederick G, Jr.** 1994. Outbreak of *Mycoplasma iowae* infection in commercial turkey poults. Avian Dis. **38**:905–909.
32. **Tully JG, Rose DL, Whitcomb RF, Wenzel RP.** 1979. Enhanced isolation of *Mycoplasma pneumoniae* from throat washings with a newly-modified cultured medium. J. Infect. Dis. **139**:478–482.
33. **Uenoyama A, Kusumoto A, Miyata M.** 2004. Identification of a 349-kilodalton protein (Gli349) responsible for cytadherence and glass binding during gliding of *Mycoplasma mobile*. J. Bacteriol. **186**:1537–1545.
34. **Wang RH, et al.** 1992. High frequency of antibodies to *Mycoplasma penetrans* in HIV-infected patients. Lancet **340**:1312–1316.
35. **Yañez A, et al.** 1999. Mycoplasma penetrans bacteremia and primary antiphospholipid syndrome. Emerg. Infect. Dis. **5**:164–167.
36. **Yoder HW, Hofstad MS.** 1964. Characterization of avian mycoplasma. Avian Dis. **8**:481–512.